ORIGINAL RESEARCH



Investigation of the effects of fluoride varnish, silver diamine fluoride and peptide P11-4 on dentin nanostructure in an *in-vitro* dentin caries model via SEM, FTIR spectroscopy and SAXS methods

Gizem Yoğurucu Değerli^{1,*}, Gunseli Güven Polat², Semra İde³, Onurcan Bülbül³

- ¹Department of Pediatric Dentistry, Faculty of Dentistry, Istanbul Health and Technology University, 34275 Istanbul, Turkey
- ²Department of Pediatric Dentistry, Hamidiye Faculty of Dental Medicine, University of Health Science, 34668 Istanbul, Turkey
- ³Department of Physics Engineering, Faculty of Engineering, Hacettepe University, 06800 Ankara, Turkey

*Correspondence

gizem.degerli@istun.edu.tr (Gizem Yoğurucu Değerli)

Abstract

Background: To evaluate and compare the structural effects of fluoride varnish, silver diamine fluoride (SDF), and peptide P11-4 on dentin nanostructure in an in vitro dentin caries model. Methods: Forty dentin discs were demineralized and treated with either SDF, fluoride varnish or P11-4. Structural changes were assessed using scanning electron microscopy (SEM), Fourier transform infrared (FTIR) spectroscopy, and smallangle X-ray scattering (SAXS) to evaluate topographical, molecular and nanoscale modifications. Results: SEM revealed morphological differences across groups: the P11-4 group showed fibrillar structures and narrowed dentinal tubules; the SDF group exhibited blocked tubules with a granular appearance; and the fluoride varnish group presented partially occluded tubules. FTIR analysis showed a reduction in Amide A and Amide I bands in the P11-4 group, suggesting enhanced interaction with dentin collagen and early-stage remineralization. In contrast, the SDF group showed higher Amide A values, indicating limited interaction with the organic matrix. These spectral shifts imply differential impacts on the preservation and reorganization of the dentin matrix. SAXS analysis confirmed that the P11-4 group exhibited the closest nanostructural resemblance to healthy dentin, whereas the SDF group showed the least similarity. Both the P11-4 and fluoride varnish groups demonstrated organized fibrillar alignment and improved mineral patterning. Conclusions: The findings suggest that P11-4, through its biomimetic action, facilitates favorable nanostructural and molecular changes in demineralized dentin. These effects may contribute to enhanced mechanical stability and long-term clinical outcomes. Broader in vivo studies are warranted to validate these results before clinical application.

Keywords

Biomimetics; Caries; Dentin; Self-assembling peptide; Preventive dentistry

1. Introduction

Dental caries, which occurs due to the localized dissolution of dental hard tissues, is a chronic disease commonly observed in society [1]. Today, instead of treating dental caries with traditional methods, it has become the main target of noninvasive treatment without cavitation. For this reason, many materials have been developed in dentistry with the increasing importance of preventive and therapeutic treatments [2, 3].

The American Pediatric Dentistry Association (AAPD) reported that the use of fluoride for the prevention and arrest of caries is effective and safe [4]. There is a consensus that the fluoride used to prevent the progression of caries has a local effect before and after its application [5]. Fluoride, which is the gold standard for preventing and arresting caries, is used in different forms [6]. Among fluoride agents, silver

diamine fluoride (SDF) can be applied directly to prevent dental caries. SDF is an alkaline solution containing silver and fluoride ions. Silver-containing compounds are used in dentistry and medicine because of their antimicrobial properties [7]. Silver nitrate, which was used as the first silver compound in dentistry, was used in the 1840s to prevent caries formation in primary teeth [8]. In the 1960s, the necessity of using silver nitrate and fluoride to achieve synergistic effects was advocated [9]. In 2014, the American Food and Drug Administration (U.S. Food and Drug Administration, FDA) approved the first SDF product for use in the United States (USA) [10].

Unlike traditional remineralization agents, P11-4, self-assembling peptide (SAP) scaffolds, which form a skeleton that helps ions precipitate, are used to arrest initial caries in the enamel [11]. SAPs are structurally assembled structures

arranged spontaneously between peptides under certain thermodynamic conditions [12]. The P11-4 peptide (Ac-Gln-Gln-Arg-Phe-Glu-Trp-Glu-Phe-Glu-Gln-Gln-NH2) can be synthesized *in vitro*. Self-assembled oligomeric β -sheet peptides; one-dimensional nanobands and nanobands form strips, and strips form fibrils, fibril pairs and fibers [13]. The predominantly anionic peptide fibers provide an appropriate surface that can control the precipitation of hydroxyapatite crystals and mimic biological macromolecules in the mammalian skeleton. Unlike traditional remineralizing agents, P11-4 is a self-assembling peptide that forms a nanofibrillar scaffold, which facilitates the guided precipitation of calcium and phosphate ions to promote biomimetic remineralization.

These supramolecular scaffolds replicate the natural extracellular matrix and enable hydroxyapatite crystal nucleation under physiological conditions [11, 14]. Numerous *in vitro* studies have reported increases in surface microhardness and improved enamel remineralization following P11-4 application [15, 16]. P11-4 is frequently used in peptide-based remineralization studies, and in studies using P11-4, the initial lesions were healed, no side effects occurred, and the resulting fiber structure had high biocompatibility [17].

While the efficacy of P11-4 has been well documented in early enamel lesions, its effects on dentin tissue remain less explored. Unlike enamel, dentin presents a more complex structure, composed of collagen fibrils and open tubules, making its remineralization more challenging [18]. As such, novel materials capable of interacting with both the organic and inorganic components of dentin are of growing interest. Most studies have focused solely on surface hardness or mineral content; however, in-depth analysis at multiple structural levels is required to fully assess remineralization outcomes. Good nanostructural alignment observed in the P11-4 and fluoride varnish groups reflects the reorganization of collagen and mineral interfaces, which may indicate early-stage tissue recovery and functional remineralization.

The aim of this study was to evaluate the topographic, molecular, and nanostructural changes induced by these agents in demineralized dentin. To this end, this *in vitro* study employed scanning electron microscopy (SEM) for surface characterization, Fourier transform infrared (FTIR) spectroscopy for molecular composition, and small-angle X-ray scattering (SAXS) for nanoscale analysis. These complementary techniques enable a comprehensive evaluation of the structural and biomimetic potential of SDF, fluoride varnish, and P11-4 in the context of dentin.

2. Materials and methods

2.1 Sample size calculation

The study's power was calculated using power analysis software (G*Power V. 3.1.9.2 program, University of Düsseldorf, Düsseldorf, NRW, Germany) to determine the number of samples [19]. Accordingly, at a significance level of $\alpha=0.05$, when the sample size for each group was set at 10, the test power was determined to be 95%. Considering a 20% loss rate, it was decided to include a total of 40 dentin sections in the study, with 10 dentin sections in each group.

2.2 Dentin disk preparation

Our study was designed to be conducted using 40 dentin sections prepared from extracted human teeth. Forty human permanent third molars were collected from individuals aged 18-40 years, who had undergone extractions as part of orthodontic treatment plans requiring the removal of third molars for space management or arch alignment. The teeth were extracted within one month prior to sample preparation and stored in deionized water containing 0.1% thymol at 4 °C until the start of the experiment. Sample preparation, including sectioning, demineralization, and treatment application, was completed within 7 days following tooth extraction. All structural analyses (SEM, FTIR and SAXS) were performed immediately after completion of the 28-day pH cycling protocol. Teeth with caries, restorations or fractures were excluded from the study. The protocol for this study is summarized in the flowchart shown in Fig. 1.

Forty dentin disks, each with a thickness of 1.0 mm and perpendicular to the long axis of the tooth above the cementoenamel junction, were prepared via a low-speed, water-cooled diamond saw (Mecatome T180, Presi, Grenoble, France). All the disks were free from coronal enamel or pulpal exposure. A standard smear layer was created on the coronal side of the dentin surface via silicon carbide papers with 600 grit, 800 grit and 1200 grit, followed by ultrasonic cleaning in deionized water for 60 seconds each, three times. The opposite side of each disk was coated with acid-resistant nail polish.

2.3 Demineralization and remineralization solutions

The demineralization solution contained 0.05 M acetic acid containing 2.2 mM calcium chloride dihydrate (CaCl₂·2H₂O) (Lot: D10201402205, Norateks Chemical Industry and Trade Ltd. Co., Istanbul, Turkey) and 2.20 mM monopotassium phosphate (KH₂PO₄) (Lot: D10261402205, Norateks Chemical Industry and Trade Ltd. Co., Istanbul, Turkey) and was adjusted to pH 4.4. The remineralization solution contained 1.5 mM CaCl₂·2H₂O, 0.90 mM KH₂PO₄ and 130 mM potassium chloride (KCl) (Lot: B116015062, Norateks Chemical Industry and Trade Ltd. Co., Istanbul, Turkey) and was adjusted to pH 7.0. Both materials were freshly prepared [20].

2.4 Preparation of artificial lesions

All the disks were immersed in demineralization solution for 72 h at 37 $^{\circ}$ C [20].

2.5 Experimental procedure

The demineralized dentin disks were randomly assigned to four groups (n = 10).

Group 1: P11-4 (Curodont Repair, "VARDIS, Switzerland).

Group 2: SDF (Riva Star by SDI (Southern Dental Industries), Bayswater, Australia).

Group 3 included fluoride varnish (ProShield, Allershausen, Germany).

Group 4: Negative control.

Each agent was applied in accordance with the respective manufacturer's instructions, as follows: P11-4 was applied in

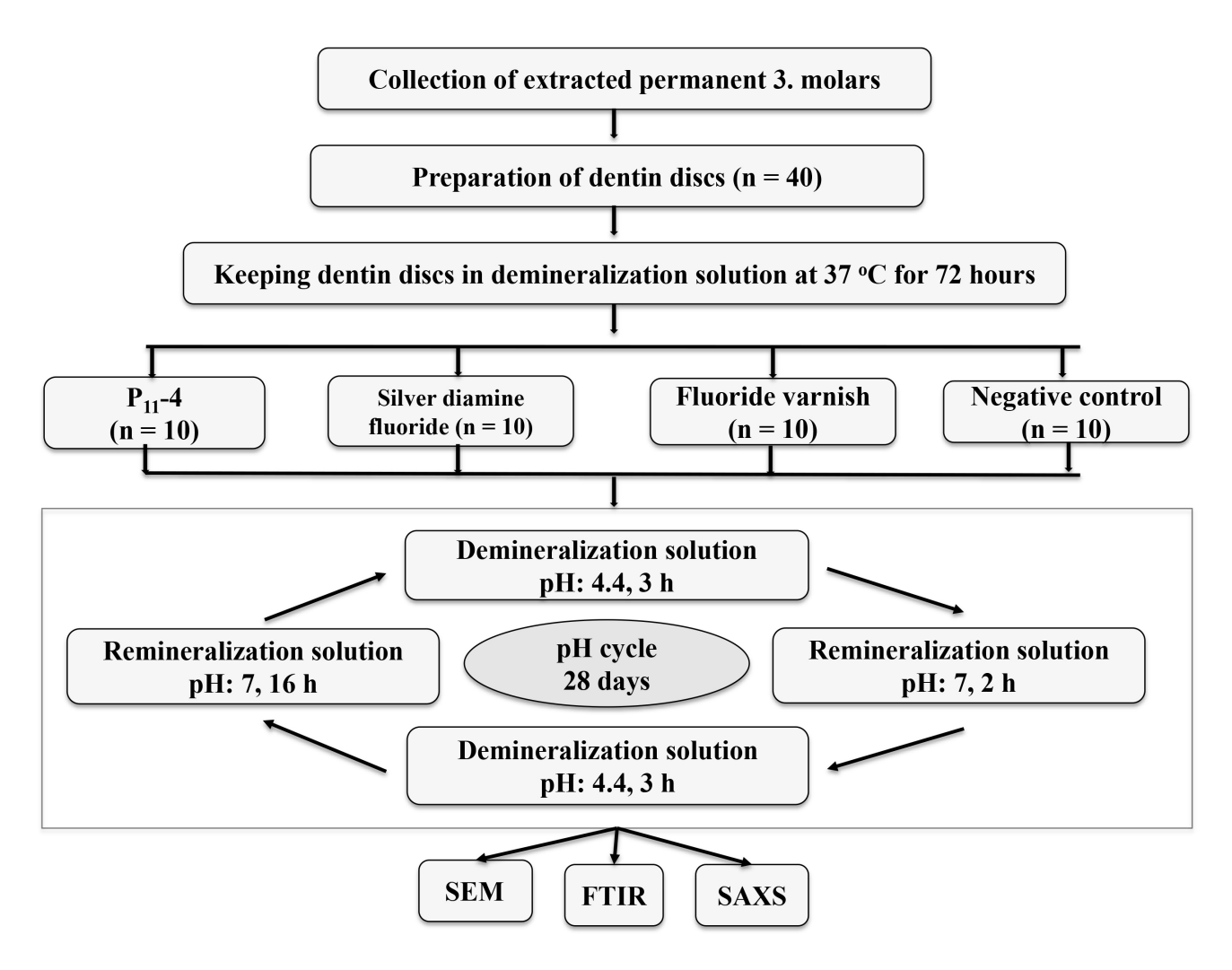


FIGURE 1. Flowchart of the experimental design. SEM: scanning electron microscopy; FTIR: Fourier transform infrared; SAXS: small-angle X-ray scattering.

a single-dose syringe and gently massaged into the surface for 5 minutes; SDF was applied using a microbrush for 1 minute, followed by the application of potassium iodide solution as recommended; and fluoride varnish was applied in a thin layer using a brush. All the disks were subjected to a 28-day pH cycling protocol that simulated clinical cariogenic conditions. Each cycle consisted of 4 hours in a demineralization solution (pH 4.4) followed by 20 hours in a remineralization solution (pH 7.0), based on modified versions of protocols widely used in artificial caries studies. This schedule mimics the daily acid challenges and recovery periods observed in the oral environment [21]. All disks were placed in individual 15 mL containers, and all solutions were freshly prepared prior to use. After completing the 28-day cycle, samples were collected for further testing.

2.6 Scanning electron microscopy (SEM)

The tooth samples used in the study were examined in the peptide P11-4, SDF, fluoride varnish and negative control groups by scanning electron microscopy (TESCAN, Brno, Czech Republic, GAIA3 + Oxford XMAX 150 EDS), which is performed on the dentin surface of the artificial caries lesion.

Morphological changes in the teeth were examined and

recorded. Before the surface coating process, an ethanol series protocol was used to completely dry the dentin sections. Each dentin section lasted 5 minutes, treated with 80% ethanol + 90% ethanol + 100% ethanol + 100% ethanol, surface cleaned and incubated at 37 °C for 24 hours until the samples were completely dry. Afterward, the surface coating was made with a platinum thickness of 5 nm. After the coating process, the sample was placed on the SEM device, the $\times 1000$ and $\times 5000$ enlargement images were examined, and the recording was completed. SEM analysis was performed on three randomly selected samples per group (n = 3), resulting in a total of 12 specimens examined.

2.7 Fourier transform infrared (FTIR) spectroscopy

Fourier-transform infrared spectroscopy (FTIR) was employed to investigate molecular-level changes in dentin specimens following remineralization treatments. The 1 mm thick dentin sections used in the study were examined with peptide P11-4, SDF and fluoride varnish and negative control groups via the Fourier Spectroscopy device "Thermo Fisher Scientific, Madison, WI, USA, Nicolet iS50". An attenuated total reflectance (ATR) crystal was used, and the central zone of each

dentin section—corresponding to the surface treated with the experimental agent—was aligned directly with the crystal for analysis. After absorption was selected as the measurement method, the samples were examined and recorded as 350 scans for 5 minutes at 4 cm⁻¹ resolution in the 4000–450 cm⁻¹ range under vacuum. For each measurement, the middle region of the dentin cross-section was carefully aligned with the diamond ATR crystal, ensuring that the treated dentin surface directly contacted the detector. The primary spectral bands of interest included phosphate (PO₄³⁻) stretching at ${\sim}1030~\text{cm}^{-1}, \text{ carbonate } (\text{CO}_3{}^{2-}) \text{ peaks around } 870 \text{ and}$ 1415 cm^{-1} , and the proteinaceous amide I ($\sim 1650 \text{ cm}^{-1}$) and amide II (~1550 cm⁻¹) bands. These peaks were analyzed to determine the carbonate-to-phosphate (C/P) and amide Ito-phosphate (Am/P) ratios, reflecting changes in mineral and organic composition. All spectra were baseline-corrected and normalized before quantitative comparison using dedicated FTIR software. FTIR analysis was conducted on three samples from each group (n = 3 per group; total n = 12).

This analysis provided complementary compositional information to SAXS structural findings, enabling a more comprehensive evaluation of biomimetic remineralization at both molecular and nanostructural levels [22].

2.8 Small-angle X-ray scattering (SAXS)

SAXS measurements were performed to evaluate nanoscale changes in the mineral and organic matrix structure of dentin specimens. Thin dentin sections ($5.0 \times 3.0 \times 1$ mm) were prepared and analyzed using a HECUS-SWAXS system (Hecus X-ray Systems, Graz, Austria), equipped with a Kratky slitcollimation setup, line collimation, and an X-ray generator operating at 50 kV and 40 mA with a Cu anode ($\lambda = 1.54 \text{ Å}$). The analyzed region corresponded to the superficial 100–200 μ m of the dentin surface that had been in contact with the remineralization agents. This area included both dentinal tubules and the surrounding intertubular matrix. This zone includes both dentinal tubules and intertubular regions. The SAXS technique provided insights into the formation, size distribution, and structural arrangement of newly formed hydroxyapatite (HAP) crystals within this surface layer. Special attention was given to determining whether these nanostructures were formed within dentinal tubules or in association with collagen fibrils in the intertubular matrix [23]. SAXS data analyses can be performed in the small q region via the obtained radius of gyration (R_a) values, and ab initio model building can be obtained directly to fit the collected data. These building models show the most likely (most dominant) morphology of the nano formations with the largest electron density difference. The distribution of these nanostructures is evidence of whether there is a homogeneous distribution within the material. The dentin structure was analyzed by referencing high-resolution transmission electron microscopy (HRTEM) images, which allow for the visualization of nanoscale formations and their distribution. The assessment was carried out in accordance with previously established protocols in the literature to enable comparison with the structural characteristics of healthy dentin. These HRTEM-based references enabled identification of structural similarities or deviations from normal dentin

ultrastructure. SAXS analysis was performed using three samples from each experimental group (n = 3), for a total of 12 dentin sections.

From a clinical perspective, a reduction in R_g values—approaching those of sound dentin—indicates the formation of densely packed, biomimetic HAP crystals. This suggests improved resistance to acid challenges and effective occlusion of dentinal tubules, which are essential for long-term structural recovery and hypersensitivity management. Healthy dentin typically exhibits a radius of gyration (R_g) in the range of 13–14 nm [24].

2.9 Statistical analysis

IBM SPSS Statistics 22 software (IBM Corp., Armonk, NY, USA) was used for the statistical analyses. The normality of data distribution was assessed using the Kolmogorov-Smirnov and Shapiro-Wilk tests, both of which indicated that the data were not normally distributed. As a result, the non-parametric Kruskal-Wallis test was employed to evaluate differences among the experimental groups. When statistically significant differences were identified, Dunn's *post-hoc* test was applied to determine which specific groups contributed to the observed differences. A Tukey *post-hoc* test was not applied, as it is appropriate for parametric data following one-way analysis of variance (ANOVA), which was not used in this study due to the non-normal distribution of the data.

3. Results

3.1 SEM analysis results

The SEM images are presented in Fig. 2. Following the creation of artificial carious lesions and completion of a 28-day pH cycling protocol, scanning electron microscopy (SEM) was performed to evaluate the dentin surfaces treated with P11-4 (Group 1), silver diamine fluoride (SDF, Group 2), and fluoride varnish (Group 3), along with an untreated control (Group 4). Images were captured at magnifications of $\times 1000$ and $\times 5000$.

3.2 FTIR spectroscopic analysis results

The FTIR spectra of experimental groups and normal dentin were analyzed across the characteristic bands associated with collagen and mineral content. The primary focus was on the Amide I (~1650 cm⁻¹), Amide A (~3300 cm⁻¹), and phosphate (~1030 cm⁻¹) bands, which are indicative of organic matrix and mineral structure. Table 1 shows the average wavenumber values for each group. Table 2 shows the comparison of Amide A and Amide I spectrum values with normal values between the groups.

The FTIR analysis revealed variations across experimental groups in the spectral regions corresponding to Amide A, Amide I and Amide II bands. In the Amide A region (N–H stretching, ~3300 cm⁻¹), the mean wavenumbers were 3294.3 cm⁻¹ (P11-4), 3296.1 cm⁻¹ (SDF), 3301.1 cm⁻¹ (fluoride varnish), and 3361.2 cm⁻¹ (negative control), compared to the normal dentin value of 3309 cm⁻¹. While the P11-4 and SDF groups showed lower values than normal, the differences were

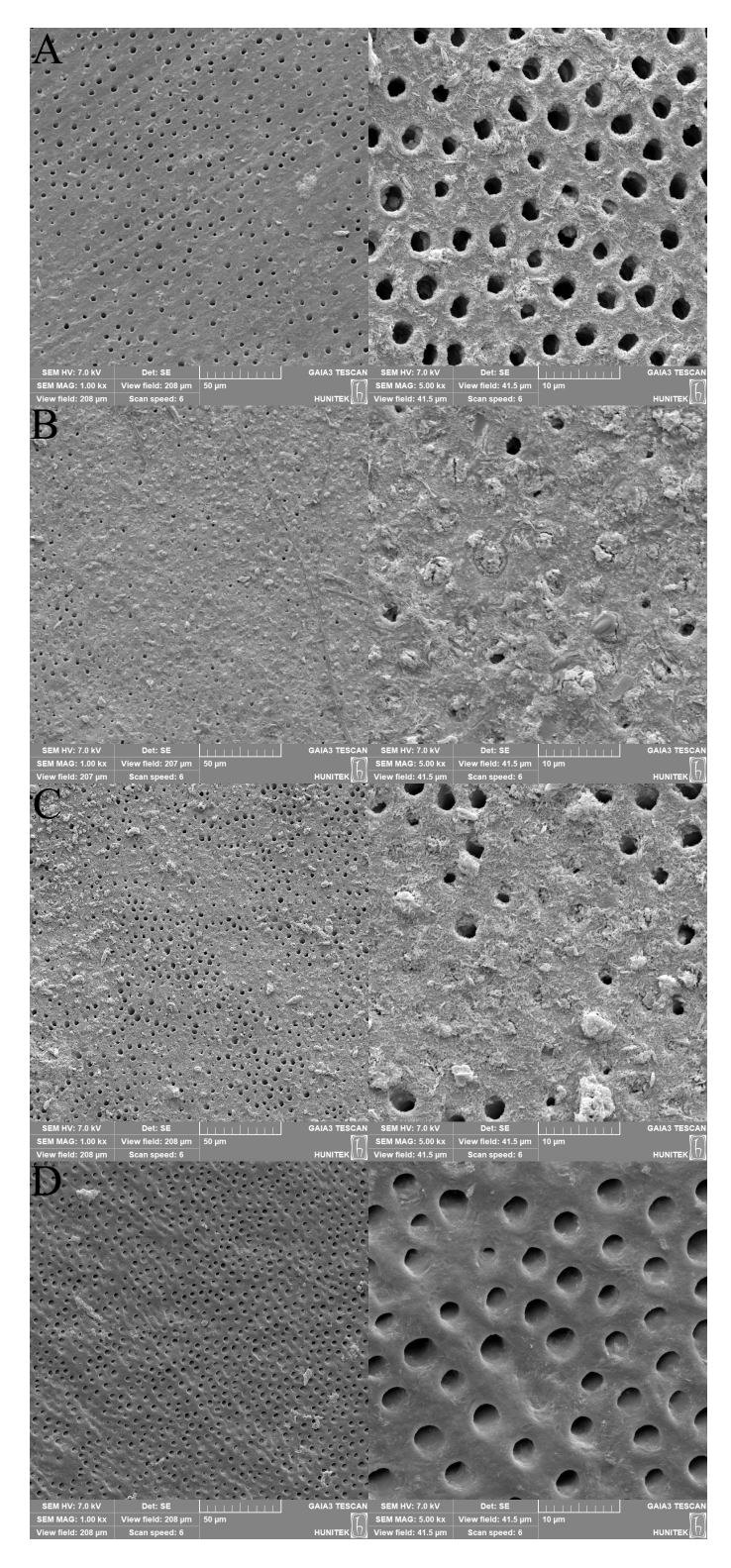


FIGURE 2. SEM images of the groups in the study. In the P11-4 group, shown in (A), narrowing of the intertubular dentin and the formation of fibrillar, fiber-like skeletal structures were observed, indicating early-stage collagen-guided remineralization. The SDF group (B) displayed predominantly occluded dentinal tubules, along with a dense and granular surface morphology suggestive of silver compound deposition and advanced mineral infiltration. In the fluoride varnish group, seen in (C), the dentinal tubules appeared partially occluded, with a visible reduction in tubule diameter and a smoother surface compared to the control group, indicating a moderate degree of surface remineralization. In contrast, the negative control group (D) exhibited irregular and deformed dentinal tubule lumens, reflecting substantial mineral loss without signs of structural recovery. These morphological differences are visually represented in Fig. 2, with each group shown at $\times 1000$ (left) and $\times 5000$ (right) magnification. SEM: scanning electron microscopy.

TABLE 1. FTIR spectrum values of the normal dentin and experimental groups (cm⁻¹).

Normal Dentin	Group 1 (P11-4)	Group 2 (SDF)	Group 3 (Fluoride varnish)	Group 4 (Negative control)	Definition of spectrum
3309 (3260–3309)	3294.3	3296.1	3301.1	3361.2	Amide A (N–H group stretching vibration)
1662 (1600–1700)	1635.1	1639.7	1690.9	1691.3	Amide I (protein C = O stretch)
1550	1542.9	1539.7	1552.1	1640.3	Amide II (protein N-H bend, C-N stretch)
1458	1458.0	1451.5	1453.4	1465.9	Organic + ν_3 CO $_3$ ²⁻ (mineral)

SDF: silver diamine fluoride; CO_3^{2-} : carbonate ion.

TABLE 2. Comparison of amide A and amide I spectrum values with normal values across groups.

	Amide A (Normal value: 3309 c	m^{-1})	Amide I (Normal value: 1662 cm ⁻¹)		
	Mean \pm SD (median)	<i>p</i> -value	$\rm Mean \pm SD (median)$	<i>p</i> -value	
Group 1	$3294.25 \pm 5.91 (3293.61)$	0.045*	$1635.07 \pm 6.30 (1632.46)$	0.018*	
Group 2	$3296.06 \pm 6.03 \ (3297.38)$	0.065	$1639.72 \pm 4.11 (1641.04)$	0.011*	
Group 3	$3301.10 \pm 9.87 (3302.41)$	0.300	$1690.94 \pm 1.51 (1691.26)$	0.001*	
Group 4	$3361.21 \pm 0.00 (3361.21)$	0.001*	$1691.26 \pm 0.00 (1691.26)$	0.001*	

One sample t test; p < 0.05. SD: standard deviation.

not statistically significant (p = 0.060, p > 0.05).

For the Amide I band (~1650 cm⁻¹), associated with C = O stretching and secondary collagen structure, the values were 1635.1 cm⁻¹ (P11-4), 1640.0 cm⁻¹ (SDF), and 1690.9 cm⁻¹ (fluoride varnish), whereas normal dentin showed a peak at 1662 cm⁻¹. Statistically significant differences were observed between the P11-4 group and both the fluoride varnish (p = 0.018) and negative control groups (p = 0.018). These shifts suggest better preservation of collagen structure in the P11-4 group.

In the Amide II region (~1550 cm⁻¹), values were 1543 cm⁻¹ (P11-4), 1540 cm⁻¹ (SDF), 1552 cm⁻¹ (fluoride varnish), and 1640 cm⁻¹ (negative control). A significant reduction was observed only in the SDF group compared to normal dentin (p < 0.05), while no significant difference was found in the P11-4 and fluoride varnish groups.

The *post-hoc* assessment results for Amide I, Amide II and Organic $+ \nu_3$ CO₃²⁻ bands are presented in Table 3.

3.3 SAXS analysis results

Small-angle X-ray scattering (SAXS) was performed to assess the nanoscale organization of remineralized dentin after treatment with P11-4, silver diamine fluoride (SDF) and fluoride varnish. The radius of gyration (R_g) values, which reflect mineral spacing and nanostructural density, were compared against the reference value for sound dentin (13.5 nm), as established in previous high-resolution transmission electron microscopy (HRTEM) studies [24]. These R_g values and nanostructural distributions were interpreted in reference to high-resolution transmission electron microscopy (HRTEM) data from previous studies, which define the expected mor-

phology and spacing of sound dentin at the nanoscale. Mean R_g values, standard deviations and statistical comparisons are presented in Table 4.

TABLE 3. Post-hoc assessment results.

Spectrum Value	Amide I	Amide II	Organic + ν_3 ${\rm CO_3}^{2-}$
	p	p	p
Group 1–Group 2	0.564	0.492	0.074
Group 1–Group 3	0.018*	0.391	0.645
Group 1–Group 4	0.018*	0.034*	0.185
Group 2–Group 3	0.074	0.122	0.185
Group 2–Group 4	0.074	0.005*	0.002*
Group 3–Group 4	1.000	0.208	0.074

*Dunn's test. p < 0.05 indicates a statistically significant difference. CO_3^{2-} : carbonate ion.

TABLE 4. Comparison of each group's R_g values with sound dentin (13.5 nm) using one-sample *t*-test.

	$Mean \pm SD (median)$	<i>p</i> -value
Group 1	14.367 ± 1.258	0.358
Group 2	13.133 ± 4.354	0.901
Group 3	15.933 ± 1.153	0.064
Group 4	16.200 ± 1.106	0.061

One sample t test. SD: standard deviation.

The P11-4 group showed R_g values closest to those of sound dentin (13.0–15.5 nm), with a mean value of 14.37 \pm 1.26 nm. One-sample t-test revealed no statistically significant difference compared to the normal dentin reference (p = 0.358), suggesting strong nanostructural similarity. In contrast, the SDF group exhibited a broader range (8.0–16.4 nm) with a mean of 13.13 \pm 4.35 nm, but also showed no significant difference (p = 0.901), likely due to high intra-group variability.

The fluoride varnish group (Group 3) displayed moderate improvements, with R_g values between 14.7 and 16.9 nm. Notably, a sample with an R_g of 14.7 nm approached the nanostructural characteristics of healthy dentin. One-sample *t*-test yielded a borderline *p*-value of 0.064, indicating a tendency toward increased mineral spacing. The negative control group exhibited higher values (mean 16.20 ± 1.11 nm, p = 0.061), reflecting disrupted and loosely packed dentin nanostructure.

SAXS analysis revealed that the greatest degree of healing toward the nanostructure of normal dentin was achieved in the P11-4 group, whereas the least healing effect was observed in the SDF-treated group. When all groups were compared, a high degree of alignment with healthy nanomorphology was observed in both the P11-4 and fluoride varnish groups, as evidenced by the consistent nanoformation distance distributions. Notably, all samples in the P11-4 group demonstrated structural improvements that closely resembled the organized, compact characteristics of sound dentin.

Fig. 3 illustrates representative nanomorphologies and size distribution profiles of the dentin samples derived from SAXS data. Each image represents a different specimen from the corresponding experimental group. These visual findings support the quantitative data by showing that the P11-4 and fluoride varnish groups exhibited more organized and condensed nanostructures compared to SDF and control.

4. Discussion

This study aimed to evaluate the structural and nanomolecular effects of P11-4 peptide, silver diamine fluoride (SDF), and fluoride varnish on demineralized dentin using SEM, FTIR and SAXS techniques. SEM analysis revealed that P11-4 promoted fibrillar structure formation and partial tubule occlusion, whereas SDF led to complete tubule sealing with granular morphology. Fluoride varnish resulted in partial occlusion with reduced tubule diameter. FTIR spectroscopy showed characteristic shifts in Amide A and I bands in all treatment groups compared to normal dentin, indicating protein matrix reorganization and altered mineral interaction. Notably, P11-4 and SDF exhibited spectral profiles closer to normal dentin. SAXS results supported these findings by demonstrating that Group 1 (P11-4) had radius of gyration (R_q) values most similar to healthy dentin, reflecting improved nanostructural organization. These multimodal results collectively suggest that P11-4 and SDF facilitate more biomimetic structural recovery in dentin than fluoride varnish.

Although the use of P11-4 peptide for dentin remineralization has shown promising results, its efficacy in dentin tissue remains underexplored compared to its more established application in enamel. Previous studies have evaluated the ability of various commercially available desensitizing agents,

including stannous fluoride, arginine-calcium carbonate complexes, and potassium nitrate, to occlude dentinal tubules via SEM analysis after brushing on roughened dentin surfaces. Compared to these agents, 11-4—used in the form of a self-assembling peptide matrix—demonstrated a superior ability to reduce the number of open tubules. In one report, P-4 treatment achieved a 12.5% reduction in hydraulic conductivity [25], suggesting improved sealing potential. In our SEM analysis, dentinal tubule narrowing was observed in the P11-4 and fluoride varnish-treated groups, with the most extensive occlusion observed in the SDF-treated group (Fig. 2).

The significance of these findings lies in their potential application in minimally invasive caries therapy. P11-4, in particular, not only induced nanofibrillar reconstruction but also maintained collagen integrity, as evidenced by red-shifted Amide bands in FTIR spectra. SAXS further demonstrated that P11-4-treated samples had compact mineral structures resembling physiological dentin, potentially offering long-term resistance to demineralization. While SDF was effective in tubule occlusion, the heterogeneity in SAXS values suggests less uniform remineralization. Fluoride varnish, although clinically common, showed limited structural restoration across all methods, reinforcing the need for novel peptide-based alternatives in dentin regeneration.

In a study in which artificial dentin caries were created in vitro via caries-free third molars extracted from patients aged 18-30 years and the P11-4 peptide was applied, the organic components of dentin, proteolytic activity, mechanical properties of the bonding interface and nanosuspension criteria for dentin affected by artificial caries were evaluated. In this study, atomic force microscopy revealed that P11-4 bound to collagen type I fibers, increased their width from 214 \pm 4 nm to 308 \pm 5 nm (p < 0.0001) and increased the resistance of collagen type I fibers to the proteolytic activity of collagenases. The application of P11-4 to caries-affected dentin increased the microtensile bond strength of the bonding interface (p <0.0001), reaching values close to those of intact dentin and decreasing the proteolytic activity in the hybrid layer. As a result, P11-4 increased the resistance of collagen fibers to proteolysis by interacting with collagen type I and improved the stability of the hybrid layer formed by dentin affected by artificial caries [26].

There are very few studies examining the clinical efficacy of the P11-4 peptide. In a study investigating the efficacy and safety of the material by applying the P11-4 peptide to initial caries with class V enamel lesions between 18–65 years of age, diluted P11-4 was used on the lesions for 30 seconds. The lesions were evaluated according to color, size, and progression criteria on the 4th, 8th, 30th and 180th days, and photographs were taken from the clinical controls. This study revealed that a single application had significant effects at the end of the 1st month, which continued for 6 months. When the effects at the end of the 1st and 6th s were compared, the main impact of P11-4 was observed at the end of the 1st month. The improvement started on the 8th day, but this improvement was not significant up to 30 days. P11-4 applied a single time can maintain its effect for up to 6 months [11].

A study evaluating the efficacy of P11-4 applied to interface caries via visual and radiographic examinations at the end

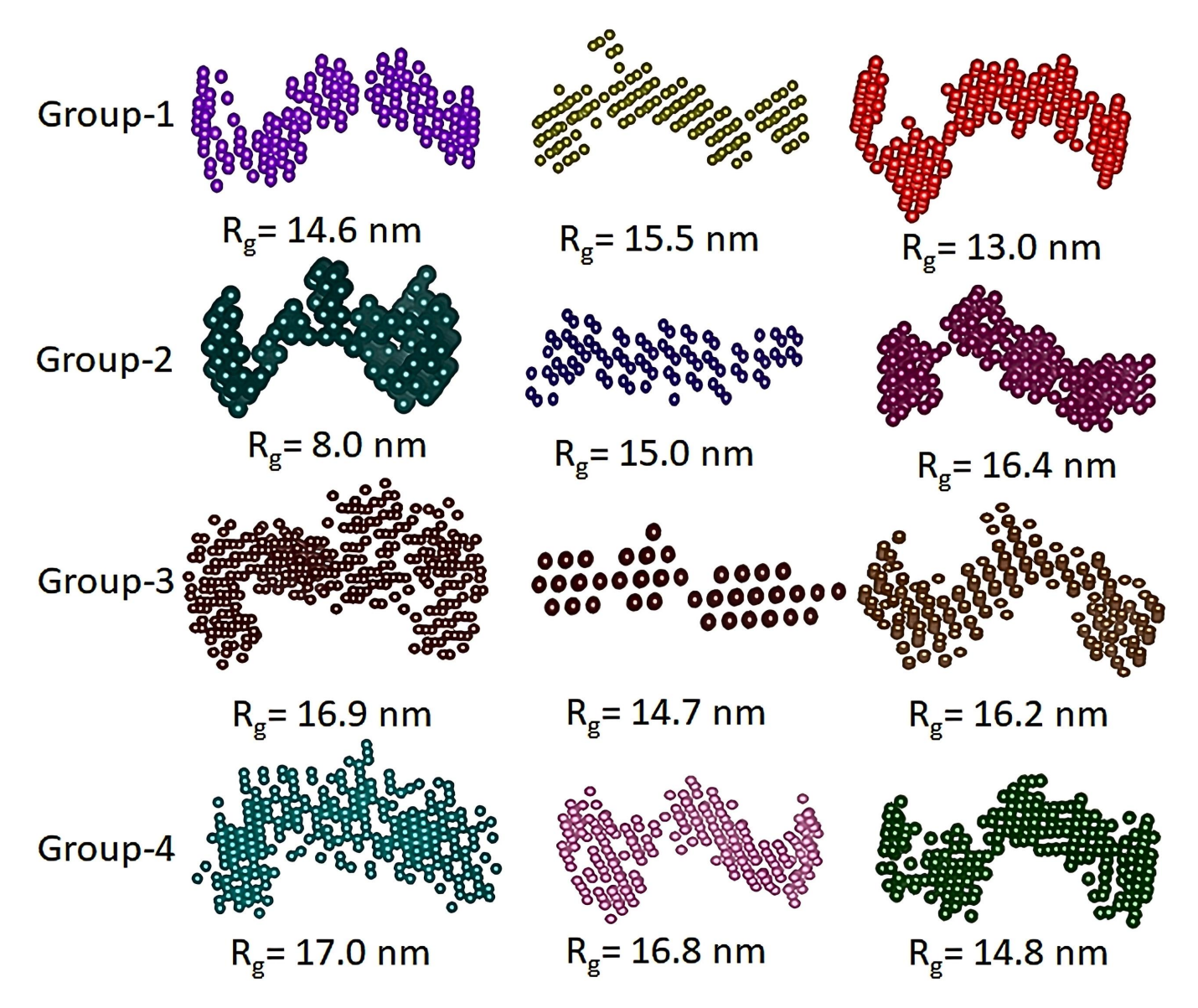


FIGURE 3. Nanomorphologies and sizes obtained in our study and the distance distributions of nano formations. Taken together, the results suggest that P11-4-treated dentin most closely resembles the nanostructure of healthy dentin, followed by fluoride varnish. Although the SDF group showed some improvement, it was less consistent in achieving biomimetic mineral organization.

of 1 year reported that 72% of caries lesions regressed and 14% arrested without progression according to the International Caries Detection and Assessment System (ICDAS) II system [27]. In our study, SAXS analysis revealed that in the P11-4-treated group, nanoscale healing was most similar to that in normal dentin tissue, and the greatest improvement in nanostructure improved after the P11-4-treated group was in the fluoride varnish-treated group.

These findings are consistent with those of the SAXS analysis, in which the biomimetic improvements of the groups treated with P11-4, SDF and fluoride varnish were evaluated, improvements were observed in all the groups, and the slightest structural improvement was observed in the group in which SDF was applied. The reason for this situation can be the precipitation of silver ions in the dentinal tubules, and SEM images also support this finding. The dentinal tubules decreased in size in the third group, where fluoride varnish,

which has been used as the gold standard for years, was applied. Although morphological narrowing of the dentin tubules was observed in the SEM images of the P11-4-treated group, it was not sufficient to evaluate the differences related to the nanobytes. According to the SAXS analysis, the best biomimetic improvement was observed in the P11-4 group. According to the FTIR analysis, while the N-H group content of the amide A band is in the range of 3400–3440 cm⁻¹, in the case of hydrogen bonding, it is observed at wavelengths with a lower band gap of 3300 cm⁻¹, and the amide A band was observed below this value in all our groups. While the alpha helix structure of the amide I band, which is the most sensitive to the secondary collagen structure, was observed at a value of 1662 cm⁻¹, values below this value were obtained in the P11-4 and SDF groups. The fact that the lowest values of both the amide A and amide I bands were observed in the P11-4treated group supports the conclusion that the best biomimetic

improvement we obtained in the SAXS analysis was in the P11-4 group. The fact that the lowest values of both the Amide A and Amide I bands were observed in the P11-4-treated group supports the conclusion that this group achieved the highest level of biomimetic nanostructural improvement.

Limitations of this study include the use of an *in vitro* model, which may not fully replicate intraoral conditions. Furthermore, the sample size for SAXS, SEM and FTIR analyses was limited to three specimens per group, which may affect the generalizability of the structural findings. Future studies with larger sample sizes and *in vivo* conditions are warranted to validate these results.

5. Conclusions

The findings of this *in vitro* study demonstrated that Curodont Repair, which contains the biomimetic peptide P11-4, contributed to structural improvements in demineralized dentin. A single application of P11-4 was associated with narrowing of dentinal tubules, partial tubule occlusion, and improved nanostructural alignment, as supported by SEM, FTIR and SAXS analyses. While these results indicate a positive structural response to P11-4, further *in vivo* and longitudinal studies are required to evaluate its long-term clinical effectiveness and applicability. Additionally, future research should explore the effects of repeated applications to determine whether enhanced dentin remineralization and tubule occlusion can be achieved. Based on the current data, P11-4 shows potential for development as a minimally invasive treatment option for dentin caries.

AVAILABILITY OF DATA AND MATERIALS

The data that support the findings of this study are available from the corresponding author—GYD, upon reasonable request.

AUTHOR CONTRIBUTIONS

GYD—contributed to the conceptualization, methodology, formal analysis, investigation, data analysis, interpretation, manuscript draft and finalization. GGP—contributed to the conceptualization, methodology, interpretation, manuscript draft and finalization. Sİ—contributed to conceptualization, data interpretation and manuscript finalization. OB—contributed to the formal analysis. All the authors read and approved the final version of the manuscript. All the authors listed in this manuscript have made substantial contributions to this study.

ETHICS APPROVAL AND CONSENT TO PARTICIPATE

The study was obtained with decision number 2021/19 from the University of Health Sciences Hamidiye Scientific Research Ethics Committee at the meeting held on 04 June 2021, recorded under approval number 46418926-050.01. Informed consent was obtained from all participants. All participants

provided consent to participate in the study.

ACKNOWLEDGMENT

Not applicable.

FUNDING

This work was supported by the Sağlık Bilimleri University Scientific Research Coordination Unit (Project Number: 2022/027) and is part of the PhD thesis of Dr. Gizem Yoğurucu Değerli.

CONFLICT OF INTEREST

The authors declare no conflict of interest.

REFERENCES

- Morawska-Wilk A, Kensy J, Kiryk S, Kotela A, Kiryk J, Michalak M, et al. Evaluation of factors influencing fluoride release from dental nanocomposite materials: a systematic review. Nanomaterials. 2025; 15: 651.
- Tsang PW, Qi F, Huwig AK, Anderson MH, Wesley D, Shi W. A medical approach to the diagnosis and treatment of dental caries. American Health Information Management Association. 2006; 47: 38–42.
- [3] Parnell C, Gugnani N, Sherriff A, James P, Beirne PV. Non-fluoride topical remineralising agents containing calcium and/or phosphate for controlling dental caries. Cochrane Database of Systematic Reviews. 2012; 3: 1–10.
- [4] American Academy of Pediatric Dentistry. Fluoride therapy. 2023. Available at: https://www.aapd.org/media/Policies_Guidelines/BP_FluorideTherapy.pdf (Accessed: 22 May 2025).
- Phyo WM, Saket D, da Fonseca MA, Auychai P, Sriarj W. In vitro remineralization of adjacent interproximal enamel carious lesions in primary molars using a bioactive bulk-fill composite. BMC Oral Health. 2024; 24: 37.
- [6] Xu GY, Zhao IS, Lung CY, Yin IX, Lo EC, Chu CH. Silver compounds for caries management. International Dental Journal. 2024; 74: 179–186.
- [7] Knight G, McIntyre J, Craig G, Mulyani, Zilm P, Gully N. An in vitro model to measure the effect of a silver fluoride and potassium iodide treatment on the permeability of demineralized dentine to Streptococcus mutans. Australian Dental Journal. 2005; 50: 242–245.
- [8] Mungur A, Chen H, Shahid S, Baysan A. A systematic review on the effect of silver diamine fluoride for management of dental caries in permanent teeth. Clinical and Experimental Dental Research. 2023; 9: 375–387.
- [9] Zheng FM, Yan IG, Duangthip D, Gao SS, Lo ECM, Chu CH. Silver diamine fluoride therapy for dental care. Japanese Dental Science Review. 2022; 58: 249–257.
- [10] American Academy of Pediatric Dentistry. Policy on the use of silver diamine fluoride for pediatric dental patients. 2023. Available at: https://www.aapd.org/media/Policies_Guidelines/P_SilverDiamine.pdf (Accessed: 22 May 2025).
- [11] Brunton PA, Davies RP, Burke JL, Smith A, Aggeli A, Brookes SJ, et al. Treatment of early caries lesions using biomimetic self-assembling peptides—a clinical safety trial. British Dental Journal. 2013; 215: E6.
- [12] Li Z, Li Y, Yin C. Manipulating molecular self-assembly process at the solid-liquid interface probed by scanning tunneling microscopy. Polymers. 2023; 15: 4176.
- [13] Kyle S, Aggeli A, Ingham E, McPherson MJ. Recombinant self-assembling peptides as biomaterials for tissue engineering. Biomaterials. 2010; 31: 9395–9405.
- [14] Hardan L, Chedid JCA, Bourgi R, Cuevas-Suárez CE, Lukomska-

- Szymanska M, Tosco V, et al. Peptides in dentistry: a scoping review. Bioengineering. 2023; 10: 214.
- [15] Schmidlin P, Zobrist K, Attin T, Wegehaupt F. In vitro re-hardening of artificial enamel caries lesions using enamel matrix proteins or selfassembling peptides. Journal of Applied Oral Science. 2016; 24: 31–36.
- [16] Dawasaz AA, Togoo RA, Mahmood Z, Azlina A, Thirumulu Ponnuraj K. Effectiveness of self-assembling peptide (P11-4) in dental hard tissue conditions: a comprehensive review. Polymers. 2022; 14: 792.
- [17] Alkilzy M, Santamaria RM, Schmoeckel J, Splieth CH. Treatment of carious lesions using self-assembling peptides. Advances in Dental Research. 2018; 29: 42–47.
- [18] Özkaya ZAG, Hidayet Z. Biomimetic remineralization of dentin. Atatürk University Journal of Faculty of Dentistry. 2020; 30: 156–166. (In Turkish)
- [19] Fortunato A, Andreassi S, Franchini C, Sciabica GM, Morelli M, Chirumbolo A, et al. Unlocking success in counseling: how personality traits moderates its effectiveness. European Journal of Investigation in Health Psychology and Education. 2024; 14: 2642–2656.
- [20] Dawasaz AA, Togoo RA, Mahmood Z, Ahmad A, Thirumulu Ponnuraj K. Remineralization of dentinal lesions using biomimetic agents: a systematic review and meta-analysis. Biomimetics. 2023; 8: 159.
- [21] Fu Y, Ekambaram M, Li KC, Zhang Y, Cooper PR, Mei ML. In vitro models used in cariology mineralisation research—a review of the literature. Dentistry Journal. 2024; 12: 323.
- [22] Lopes CDCA, Limirio PHJO, Novais VR, Dechichi P. Fourier transform infrared spectroscopy (FTIR) application chemical characterization of enamel, dentin and bone. Applied Spectroscopy Reviews. 2018; 53: 747– 769

- [23] Kline SR. Reduction and analysis of SANS and USANS data using IGOR Pro. Journal of Applied Crystallography. 2006; 39: 895–900.
- [24] Tiznado-Orozco GE, García-García R, Reyes-Gasga J. Structural and thermal behaviour of carious and sound powders of human tooth enamel and dentine. Journal of Physics D: Applied Physics. 2009; 42: 235408.
- [25] Hill R, Chen X, Lysek DA, Gillam D. An in vitro comparison of a novel self-assembling peptide matrix gel and selected desensitizing toothpastes in reducing fluid flow by dentine tubular occlusion. Journal of Dental and Maxillofacial Research. 2020; 3: 1–11.
- [26] Costa R, Reis-Pardal J, Arantes-Oliveira S, Ferreira JC, Azevedo LF, Melo P. Biomimetic remineralization strategies for dentin bond stability—systematic review and network meta-analysis. International Journal of Molecular Sciences. 2025; 26: 3488.
- [27] Schlee M, Schad T, Koch JH, Cattin PC, Rathe F. Clinical performance of self-assembling peptide P₁₁-4 in the treatment of initial proximal carious lesions: a practice-based case series. Journal of Investigative and Clinical Dentistry. 2018; 9: e12286.

How to cite this article: Gizem Yoğurucu Değerli, Günseli Güven Polat, Semra İde, Onurcan Bülbül. Investigation of the effects of fluoride varnish, silver diamine fluoride and peptide P11-4 on dentin nanostructure in an *in vitro* dentin caries model via SEM, FTIR spectroscopy and SAXS methods. Journal of Clinical Pediatric Dentistry. 2025; 49(6): 215-224. doi: 10.22514/jocpd.2025.144.